

- have carried out a microwave study of 1,1,2,2-tetrafluorocyclopropane, which yields a value of 1.47 Å for the C(1)–C(2) bond distance. The C(3)–C(1,2) bond lengths could not be determined due to the unfavorable position of the center of mass.
- (27) W. J. Hehre and J. A. Pople, *J. Am. Chem. Soc.*, **92**, 2191 (1970).
 (28) W. J. Hehre, R. F. Stewart, and J. A. Pople, *J. Chem. Phys.*, **51**, 2657 (1969); W. J. Hehre, R. Ditchfield, R. F. Stewart, and J. A. Pople, *ibid.*, **52**, 2769 (1970).
 (29) J. A. Pople and G. A. Segal, *J. Chem. Phys.*, **44**, 3289 (1966); D. P. Santry and G. A. Segal, *ibid.*, **47**, 158 (1967).
 (30) M. D. Newton, W. A. Lathan, W. J. Hehre, and J. A. Pople, *J. Chem. Phys.*, **52**, 4064 (1970).
 (31) J. A. Pople and M. S. Gordon, *J. Am. Chem. Soc.*, **89**, 4253 (1967); L. Radom, W. J. Hehre, and J. A. Pople, *ibid.*, **94**, 2371 (1972).
 (32) P. C. Hariharan and J. A. Pople, *Chem. Phys. Lett.*, **16**, 217 (1972).
 (33) R. S. Mulliken, *J. Chem. Phys.*, **23**, 1833, 1841, 2338, 2343 (1955).
 (34) A. D. Walsh, *J. Chem. Soc.*, 2260, 2266, 2288, 2296, 2301 (1953); A. D. Walsh, *Prog. Stereochem.*, **1**, 1 (1954).
 (35) J. M. Lehn and G. Wipff, *Theor. Chim. Acta*, **28**, 223 (1973); *Chem. Phys. Lett.*, **15**, 450 (1972).
 (36) M. D. Newton and J. M. Schulman, *J. Am. Chem. Soc.*, **94**, 767 (1972).
 (37) R. P. Feynman, *Phys. Rev.*, **56**, 340 (1939); H. Hellmann, "Einführung in die Quantenchemie", Franz Deuticke, Leipzig, E. Germany, 1937, pp 285ff.
 (38) B. M. Deb, *J. Am. Chem. Soc.*, **96**, 2030 (1974).
 (39) H. Nakatsuji, *J. Am. Chem. Soc.*, **95**, 345, 354 (1973).

On the Theory of Phase-Transfer Catalysis¹

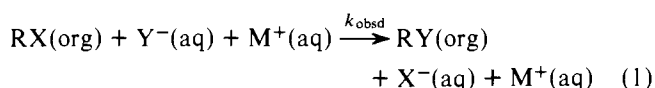
John E. Gordon* and Raymond E. Kutina

Contribution from the Department of Chemistry, Kent State University,
 Kent, Ohio 44242. September 10, 1976

Abstract: Two-phase reactions run under phase-transfer catalysis (PTC), such as $RX(\text{org}) + Y^-(\text{aq}) \rightarrow RY(\text{org}) + X^-(\text{aq})$, are treated as sums of the rate-limiting, homogeneous reactions $RX(\text{org}) + Y^-(\text{org}) \rightarrow RY(\text{org}) + X^-(\text{org})$ and the rapidly established liquid ion-exchange equilibria $Y^-(\text{aq}) + Q^+X^-(\text{org}) (K_{Y/X^{\text{sel}}}) \rightleftharpoons X^-(\text{aq}) + Q^+Y^-(\text{org})$. It is shown that the kinetic behavior is determined by $K_{Y/X^{\text{sel}}}$: $K_{Y/X^{\text{sel}}} < 1$ leads to "catalyst poisoning" and no simple rate law; $K_{Y/X^{\text{sel}}} = 1$ gives standard second-order behavior; $K_{Y/X^{\text{sel}}} > 1$ often leads to pseudo-first-order behavior. The efficiency of PTC, measured by the quotient of the observed rate constant and an intrinsic rate constant for the reaction conducted homogeneously in an appropriate solvent, $k_{\text{obsd}}/k_{\text{int}}$, is separated into two factors. The *physical* factor results from the inhomogeneous distribution of solutes and depends upon the concentrations of Y^- , X^- , catalytic (Q^+), and inert (M^+) cations, the volume fraction of the organic phase, and $K_{Y/X^{\text{sel}}}$ (and consequently the identity of solvent, Q^+ , Y^- , and X^-). The *chemical* factor is determined primarily by ion-association and -solvation effects on Y^- in the organic phase and thus depends on identity of solvent, Y^- , and Q^+ and the ionic concentrations. Analytical expressions for the physical efficiency are derived for three cases: I, no X^- present initially; II, X^- present but $K_{Y/X^{\text{sel}}} = 1$; III, X^- present and $K_{Y/X^{\text{sel}}} \neq 1$. A collection of values of $K_{Y/X^{\text{sel}}}$ for anions of interest is presented for rough quantitative prediction of rate laws and efficiencies. The effects of PTC on rate and equilibrium in reversible second-order systems is also examined. When nucleophile Y^- is generated in situ from $YH + OH^-$ the rapid distribution equilibria involve four species (YH , Y^- , OH^- , X^-) in two phases, but the rate law can still be treated numerically; the conditions for simple second-order kinetic behavior are determined.

Phase-transfer catalysis (PTC) increases the rate of reactions between nonelectrolyte substrates located in organic phases and ionic reagents located in a contacting aqueous phase.² The catalytic agents are salts of large organic ions. The reaction rates observed for a given reaction in these systems are determined in part by the chemical factors familiar in homogeneous media: an intrinsic rate modified by ion-solvation and ion-association forces. But in part the observed rates are governed by a more physical factor—the heterogeneity of the system and the distribution of the ions between the phases. This article investigates the nature of this distribution and analyzes the dependence of the catalytic efficiency upon it.

We limit consideration to second-order reactions and illustrate these, with little loss in generality, by the S_N2 reaction of substrate $R-X$ with nucleophile Y^- . We identify the organic phase as (org), the aqueous phase as (aq), the inorganic counterion of reactant Y^- and product X^- as M^+ , and the catalytic organic cation (most often a quaternary ammonium cation) as Q^+ . The overall reaction is then

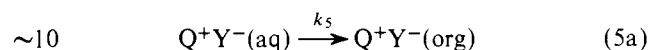
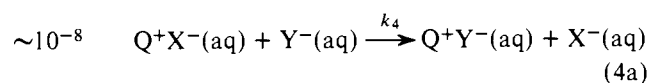
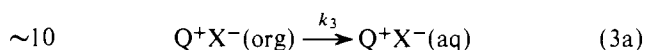
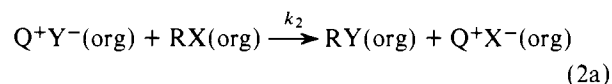


Phase-Transfer Catalysis as Liquid Ion-Exchange Catalysis. Three basic mechanisms³ for PTC are shown below. Model A is a literal interpretation of the diagram first offered by Starks.^{2,5} Model B is A with a different aqueous-phase reference state. Model C is that written in Starks's second paper.⁶

Each model's equations sum to the overall reaction, eq. 1. Models A and B maintain the electroneutrality of the phases by anion-plus-cation transport (Figure 1a), model C by anion vs. anion transport (Figure 1b).

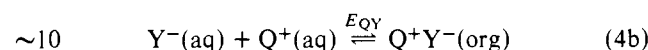
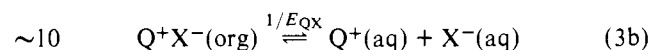
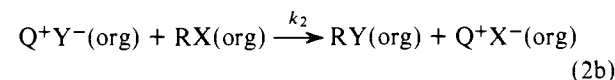
Model A

$t_{1/2}, s$



Model B

$t_{1/2}, s$



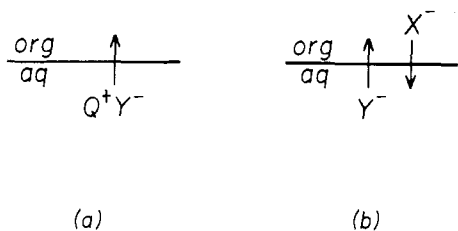
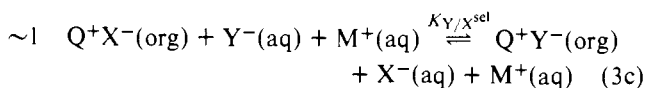
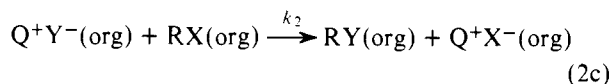


Figure 1. Alternative modes of anion transport between phases.

Model C

$t_{1/2, S}$



Using equations for diffusion control,⁷ one can estimate⁸ the probable maximum half-lives for reactions 3a–5a, 3b, and 4b; these values are shown to the left of the equations. The $t_{1/2}$ for liquid ion-exchange reactions 3c are known from the response times of ion-selective electrodes to be of the order of magnitude of 1 s.⁹ These various ionic redistribution times can be compared with a typical half-life of ca. 10^3 s for reaction 2. Each of the three models predicts reaction 2 to be rate limiting, and the three are kinetically indistinguishable by measurements on the $RX \rightarrow RY$ reaction. In accord with these models, observed rates of reaction under PTC are independent of the effectiveness of contact between the phases over a broad range of stirring speeds.^{2,10,11}

While relaxation spectrometric measurements will presumably eventually settle the choice between models C vs. A and B, this has no bearing on the kinetics of the $RX \rightarrow RY$ reaction, in which the anion redistribution (eq 3–5) can be treated, by the most efficient means available, as an instantaneous equilibration. Equations 3b and 4b express the anion distribution equilibrium in terms of the extraction constants, E_{sal} , employed by Brändström;⁴ eq 3c represents it as a liquid anion-exchange equilibrium. The relationship of E_{sal} to the ion-exchange selectivity coefficient, K^{sel} , is given by

$$K_{Y/X}^{sel} = \frac{c_{aq} X^- c_{org}^{QY}}{c_{aq} Y^- c_{org}^{QX}} = \frac{E_{QY}}{E_{QX}} \quad (6)$$

in which c_{aq} and c_{org} are concentrations in the aqueous and organic phases. E_{QY} and E_{QX} together contain more information than $K_{Y/X}^{sel}$, but values of E_{sal} are scarce.⁴ One really needs only the ratio of E_{sal} values to define the PTC system for most purposes, and $K_{Y/X}^{sel}$ values are more available (next section).

There are two more reasons why it is useful to look at PTC as liquid ion-exchange catalysis. That view emphasizes the analogy with catalysis by ion-exchange resins, about which considerable is known.¹² And it allows one to appropriate the information available for liquid ion-exchange equilibria^{7a,9,13} for use in PTC systems.

Selectivity Coefficients. Values of $K_{Y/X}^{sel}$ for a variety of anions in several systems have become available in the last few years as a by-product of work on ion-selective electrodes, which are commonly liquid ion-exchange electrodes. The potential developed by an anion-exchange membrane electrode, Q^+Y^- , in the presence of foreign anion X^- is directly related to the selectivity coefficient $K_{Y/X}^{sel}$ (eq 3c).^{9,14,15} These values are not terribly accurate in many instances, but they can be obtained rapidly and are applicable to all ions; consequently they are well suited for semiquantitative guidance in planning and evaluating PTC experiments. A variety of these values is

cation	$Q_{1,1,1,1,1,1}^+$	$Q_{1,1,1,1,1,1}^+$	$Q_{1,1,1,1,1,1}^+$	$Q_{1,1,1,1,1,1}^+$	$Q_{1,1,1,1,1,1}^+$	$Ni(o-phen)_3^{2+}$
solvent	1-decanol	$CHCl_3$	CH_2Cl_2	$CHCl_3$	$C_6H_5NO_2$	
6				<chem>O=[N+]([O-])c1ccc(cc1)[N+](=O)[O-]</chem>		
5				<chem>O=[N+]([O-])c1ccc(cc1)[N+](=O)[O-]</chem>		<chem>[O-]c1ccc(cc1)[O-]</chem>
4				<chem>[O-]c1ccc(cc1)[O-]</chem>		
3	<chem>[O-]c1ccc(cc1)[O-]</chem>	<chem>[O-]c1ccc(cc1)[O-]</chem>		<chem>[O-]c1ccc(cc1)[O-]</chem>		
2	<chem>[O-]c1ccc(cc1)[O-]</chem>	<chem>[O-]c1ccc(cc1)[O-]</chem>		<chem>[O-]c1ccc(cc1)[O-]</chem>		
1	<chem>[O-]c1ccc(cc1)[O-]</chem>	<chem>[O-]c1ccc(cc1)[O-]</chem>		<chem>[O-]c1ccc(cc1)[O-]</chem>		
0	<chem>[O-]c1ccc(cc1)[O-]</chem>	<chem>[O-]c1ccc(cc1)[O-]</chem>		<chem>[O-]c1ccc(cc1)[O-]</chem>		
-1	<chem>[O-]c1ccc(cc1)[O-]</chem>	<chem>[O-]c1ccc(cc1)[O-]</chem>		<chem>[O-]c1ccc(cc1)[O-]</chem>		
-2	<chem>[O-]c1ccc(cc1)[O-]</chem>	<chem>[O-]c1ccc(cc1)[O-]</chem>		<chem>[O-]c1ccc(cc1)[O-]</chem>		
Series	(1)	(2)	(3)	(4)	(5)	(6)
Reference	(16)	(17)	(18)	(18)	(4)	(18)

Figure 2. Logarithms of selectivity coefficients (eq 3c, 6) for exchange of anions vs. Cl^- .

shown, as $\log K_{Y/Cl}^{sel}$, in Figure 2.^{16–18} For estimation of $K_{A/B}^{sel}$ notice that $\log K_{A/B}^{sel} = \log (K_{A/Cl}^{sel} - K_{B/Cl}^{sel})$.

The anion order is often closely similar from one system to the next. The range of $K_{Y/X}^{sel}$ is several powers of ten greater in some systems than others, however. The larger $K_{Y/X}^{sel}$ values in the $Ni(o-phen)_3^{2+}$ /nitrobenzene system may be of value in some PTC applications.

Second-Order Rate Laws. Equation 7 is the rate expression written for the system of eq 2c + eq 3c = eq 1 by an observer who knows the system is heterogeneous and knows its composition. Equation 8 is the rate expression written by a primitive¹⁹ observer who is unaware that the phase boundary exists. The symbols are those of eq 1–4; unsubscripted concentrations are computed using the volume of the system as a whole ($V_{org} + V_{aq}$).

$$dc_{org}^{RY}/dt = k_{org} c_{org}^{RX} c_{org}^{Y^-} \quad (7)$$

$$dc^{RY}/dt = k_{obsd} c^{RX} c^{Y^-} \quad (8)$$

Starks and Owens⁶ integrated the rate law and showed that in general second-order kinetics is not obeyed. We have found it useful to study the rate profiles using computerized numerical treatment of the differential form of the rate law (eq 7) together with eq 2c and 3c (see Computation Section). With minor changes the routines can handle more complex systems in which further equilibria are superimposed; three of these are discussed below. Figure 3 shows the basic dependence of the rate profile on $K_{Y/X}^{sel}$. A linear second-order plot is observed only for $K_{Y/X}^{sel} = 1$ (curve c) (a formal proof is also readily deduced). Other values of $K_{Y/X}^{sel}$ distort the manner in which $c_{org}^{Y^-}$ falls off with time. $K_{Y/X}^{sel} > 1$ maintains unnaturally large concentrations of Y^- in the organic phase and gives the appearance of autocatalysis (curves a and b). $K_{Y/X}^{sel} < 1$ concentrates product anion X^- in the organic phase; $K_{Y/X}^{sel}$ below 0.1 effectively stalls the reaction. This "catalyst poisoning" effect is well known in practice.^{2,6,10,11} Figure 4 shows the limited success that can be expected in overcoming

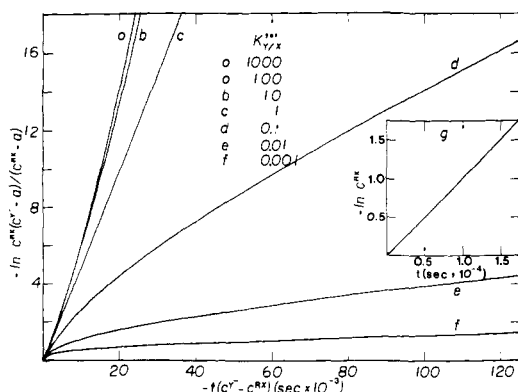


Figure 3. Rate profiles for PT catalyzed reaction 1: (a)–(f) second-order plots with $k_{\text{org}} = 10^{-3} \text{ M}^{-1} \text{ s}^{-1}$, $c_0^{\text{RX}} = 1 \text{ M}$, $c_0^{\text{Y}^-} = 2 \text{ M}$, $c_0^{\text{X}^-} = 0$, $c_{\text{org}}^{\text{Q}^+} = 0.1$, $n = 50$, and $K_{\text{Y}/\text{X}}^{\text{sel}}$ as shown; (g) pseudo-first-order plot of the data of curve (a).

catalyst poisoning by increasing the catalyst concentration at $K_{\text{Y}/\text{X}}^{\text{sel}} = 0.01$.

When the data of curve a in Figure 3 ($K_{\text{Y}/\text{X}}^{\text{sel}} \geq 100$) are replotted as a pseudo-first-order process, the linear plot g (inset) is obtained. Pseudo-first-order behavior is observed whenever the magnitude of $K_{\text{Y}/\text{X}}^{\text{sel}}$ and any excess of Y^- , combined, suffice to hold $c_{\text{org}}^{\text{Y}^-}$ effectively constant. One can get good pseudo-first-order plots under some unusual conditions in such a system—with a deficiency of Y^- , if $K_{\text{Y}/\text{X}}^{\text{sel}}$ is sufficiently large, as shown in Table I. Of course, the linear first-order plots at large $K_{\text{Y}/\text{X}}^{\text{sel}}$ and small $\text{Y}^-:\text{RX}$ display a break; the rate falls off abruptly when the remaining Y^- is insufficient to keep all the organic-phase ionic sites in the Y^- form (i.e., when remaining $\text{Y}^- < \text{Q}^+$).

How do $K_{\text{Y}/\text{X}}^{\text{sel}}$ and other variables influence the rate of reaction? This question is attacked in the next section by applying a general theory of multidomain reactions due to Morawetz.²⁰

Catalytic Efficiency. The efficiency of phase-transfer catalysis, q , is the ratio of the observed catalytic rate to the rate that would be observed in an otherwise similar, homogeneous system in which all chemical and solute-solute interactions involving the catalyst are absent. If the native system consists of an aqueous phase containing only MY and an immiscible organic phase containing only RX , this definition assigns an efficiency of zero to the native system without catalyst and an efficiency of unity to a catalyst whose effect is simply to homogenize the two phases, introduce no ion association, and give the rate constant for the $\text{RX} + \text{Y}^-$ reaction a value (k_{ini}) typical of the reaction in a dipolar aprotic solvent in which ion association is absent and anion solvation minimal.

It is useful to separate the purely physical contributions to q (those associated solely with the two-phase nature of the system) from the remaining “chemical” contributions. This is accomplished by the equation

$$q = k_{\text{obsd}}/k_{\text{ini}} = q_{\text{phys}} \cdot q_{\text{chem}} = (k_{\text{obsd}}/k_{\text{org}}) \cdot (k_{\text{org}}/k_{\text{ini}}) \quad (9)$$

in which k_{obsd} is that of eq 8 and 1, k_{org} is the ordinary, homogeneous, second-order rate constant for the $\text{RX} + \text{QY}$ reaction in the organic phase (eq 2), and k_{ini} is the intrinsic rate constant defined above. In most water-immiscible organic solvents q_{chem} will be dominated by ion association of Y^- with Q^+ , which depresses k_{org} and produces $q_{\text{chem}} < 1$. In this case q_{chem} can be analyzed using a theory developed elsewhere.²¹ Such depression of PTC efficiency with increasing organic-phase ion association (decreasing electrostatic radius of Q^+) is clearly illustrated in the study of Herriott and Picker.¹⁰ Here

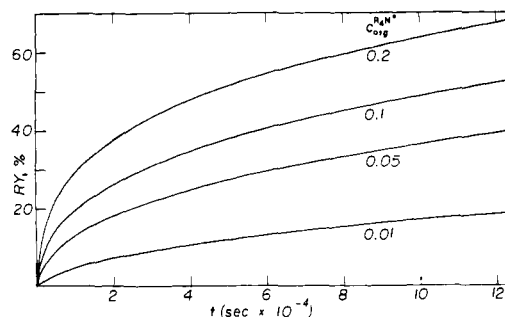


Figure 4. Percent completion of reaction 1 vs. time with $K_{\text{Y}/\text{X}}^{\text{sel}} = 0.01$, $c_0^{\text{Y}^-} = 2 \text{ M}$, $c_0^{\text{RX}} = 1 \text{ M}$, $c_0^{\text{X}^-} = 0$, and $c_{\text{org}}^{\text{Q}^+}$ as shown.

Table I. Sufficient Conditions for Observation of Pseudo-First-Order Kinetics

$K_{\text{Y}/\text{X}}^{\text{sel}}$	Minimum $\text{Y}^-:\text{RX}$ for linearity
1	10
1.33	8
2	4
10	2
100	0.8
1000	<0.4

we take up next the analysis of the contribution of q_{phys} to the observed efficiencies.

The rates calculated by the naive and sophisticated observers using eq 7 and 8 must be equal. This condition gives eq 10, in which v_i is the volume fraction of the i th phase, and c_0 is an initial concentration.

$$\frac{k_{\text{obsd}}}{k_{\text{org}}} = \frac{\sum_{i=1}^n c_i^{\text{RX}} c_i^{\text{Y}^-} v_i}{\sum_{i=1}^n c_i^{\text{RX}} v_i \sum_{i=1}^n c_i^{\text{Y}^-} v_i} \quad (10a)$$

$$= \frac{c_{\text{org}}^{\text{Y}^-}}{v_{\text{org}} c_0^{\text{Y}^-}} \quad (\text{initial rates or } K_{\text{Y}/\text{X}}^{\text{sel}} = 1) \quad (10b)$$

This expression for q_{phys} can be evaluated for several cases more interesting than the restricted condition of eq 10b.

Case I: $c_0^{\text{X}^-} = 0$, all values of $K_{\text{Y}/\text{X}}^{\text{sel}}$.

$$\frac{k_{\text{obsd}}}{k_{\text{org}}} = \frac{c_{\text{org}}^{\text{Q}^+}}{v_{\text{org}}(c_{\text{org}}^{\text{Q}^+} v_{\text{org}} + c_{\text{aq}}^{\text{M}^+} v_{\text{aq}})} = \frac{c_{\text{org}}^{\text{Q}^+}}{v_{\text{org}} c_0^{\text{Y}^-}} \quad (\text{generally}) \quad (11a)$$

$$= \frac{4c_{\text{org}}^{\text{Q}^+}}{c_{\text{org}}^{\text{Q}^+} + c_{\text{aq}}^{\text{M}^+}} = \frac{4c^{\text{Q}^+}}{c^{\text{Q}^+} + c^{\text{M}^+}} \quad (\text{for } v_{\text{org}} = v_{\text{aq}}) \quad (11b)$$

When product anion (X^-) is absent at the beginning of the reaction q_{phys} is independent of $K_{\text{Y}/\text{X}}^{\text{sel}}$, inversely proportional to v_{org} , and proportional to the fraction of all the anion sites that are located in the organic phase. The physical significance of eq 11a is best visualized by setting $v_{\text{org}} = v_{\text{aq}} = 0.5$ (eq 11b) and carrying out the following thought experiment. Start with RX and Y^- homogeneously distributed throughout the system, then concentrate them into the organic phase; this increases k_{obsd} by a factor of $2 \times 2 = 4$. Leave RX there, but distribute Y^- over all the cationic sites [M^+ in (aq), Q^+ in (org)]. This reduces k_{obsd} by a factor of $\text{Q}^+ / (\text{Q}^+ + \text{M}^+)$; both factors of eq 11b are now accounted for.

Consider a practical illustration. Observed PTC rate constants for a series of different catalysts are to be compared. Since the catalyst concentration also varies through the suite

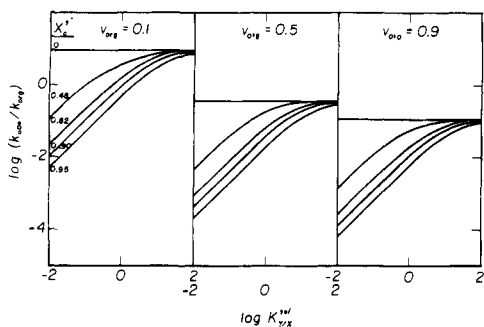


Figure 5. Catalytic efficiency for case III (eq 14) vs. selectivity coefficient (eq 3c) at the initial anion fractions of X^- and volume fractions of the organic phase shown.

of k_{obsd} values, these are recalculated to a constant catalyst concentration via multiplication by an appropriate factor (the proportionality of k_{obsd} to Q^+ concentration having been already established). Note, however, that it follows from, say, eq 11b that the ratio of any two k_{obsd} multiplied by the catalyst concentration ratio does not give just the ratio of k_{org} , ready for chemical interpretation in terms of ion association, etc., but rather this ratio perturbed by a further "physical" factor that is irrelevant to such interpretation.

$$\frac{k_{\text{obsd}}^a}{k_{\text{obsd}}^b} = \frac{k_{\text{org}}^a}{k_{\text{org}}^b} \cdot \frac{c_a^{Q^+}}{c_b^{Q^+}} \cdot \frac{(c_b^{Q^+} + c_b^{M^+})}{(c_a^{Q^+} + c_a^{M^+})} \quad (12a)$$

$$\frac{k_{\text{obsd}}^a}{k_{\text{obsd}}^b} \cdot \frac{c_b^{Q^+}}{c_a^{Q^+}} = \frac{c_b^{Q^+} + c_b^{M^+}}{c_a^{Q^+} + c_a^{M^+}} \cdot \frac{k_{\text{org}}^a}{k_{\text{org}}^b} \quad (12b)$$

In the extensive series of Herriott and Picker¹⁰ the maximum ratio of catalyst concentrations (~ 300) results in a minimum value of the factor $(c_b^{Q^+} + c_b^{M^+})/(c_a^{Q^+} + c_a^{M^+})$ of 0.96, which could decently be neglected. However, if such a comparison were made for smaller or variable concentrations of M^+ (i.e., $c_a^{M^+} \neq c_b^{M^+}$), a substantial misinterpretation could result.

Case II: $c_0^{X^-} \neq 0$, $K_{Y/X}^{\text{sel}} = 1$.

$$\frac{k_{\text{obsd}}}{k_{\text{org}}} = \frac{c_{\text{org}}^{Q^+}}{v_{\text{org}}(c_0^{Y^-} + c_0^{X^-})} = \frac{c_{\text{org}}^{Q^+}}{v_{\text{org}}c_0^{Y^-}} \cdot X_0^{Y^-} \quad (13)$$

The presence of X^- at the beginning of the reaction reduces q_{phys} by an additional factor, $X_0^{Y^-}$, which is the fraction of all anions (present at the beginning of the reaction) that are Y^- —provided $K_{Y/X}^{\text{sel}} = 1$. Otherwise we have the much more complex case III, discussed below.

Case III: $c_0^{X^-} \neq 0$, $K_{Y/X}^{\text{sel}} \neq 1$.

$$\frac{k_{\text{obsd}}}{k_{\text{org}}} = \frac{1}{2v_{\text{org}}^2(1 - K_{Y/X}^{\text{sel}})c_0^{Y^-}} \times \{c_0^{Y^-} - K_{Y/X}^{\text{sel}}(c_0^{Y^-} + c_0^{Q^+}) - c_0^{M^+} + [K_{Y/X}^{\text{sel}2}(c_0^{Y^-2} + c_0^{Q+2}) + (1 - K_{Y/X}^{\text{sel}})c_0^{Y^-}(c_0^{Y^-} + 3K_{Y/X}^{\text{sel}}c_0^{Q^+} - c_0^{M^+}) + K_{Y/X}^{\text{sel}}c_0^{Q^+}c_0^{M^+}]^{1/2}\} \quad (14)$$

Dependence on $K_{Y/X}^{\text{sel}}$ has appeared, and the response of q_{phys} to the experimental variables is best visualized graphically. Initially present X^- depresses the efficiency by degrees that are dependent on $K_{Y/X}^{\text{sel}}$ (Figures 5 and 6).

Partitioning of some Q^+ into the aqueous phase depresses the efficiency to an extent (independent of $K_{Y/X}^{\text{sel}}$) given by eq 15. This effect of K_D does not interact with that of $c_0^{X^-}$, but it is magnified at small v_{org} (Figure 7).

$$K_D = c_{\text{org}}^{Q^+}/c_{\text{aq}}^{Q^+} \quad (15a)$$

$$\frac{k_{\text{obsd}}}{k_{\text{org}}} = \frac{c_0^{Q^+}}{v_{\text{org}}^2(c_0^{Q^+} + c_0^{M^+})} \left(1 - \frac{v_{\text{aq}}}{K_D v_{\text{org}} + v_{\text{aq}}}\right) \quad (15b)$$

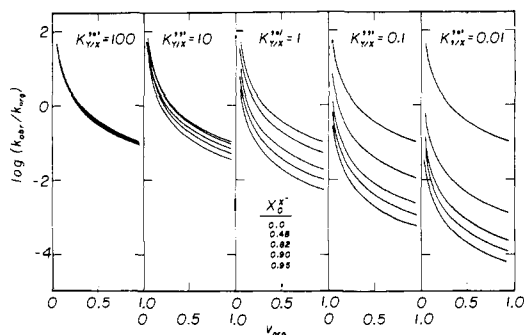


Figure 6. Catalytic efficiency for case III (eq 14) vs. organic-phase volume fraction, other variables as shown.

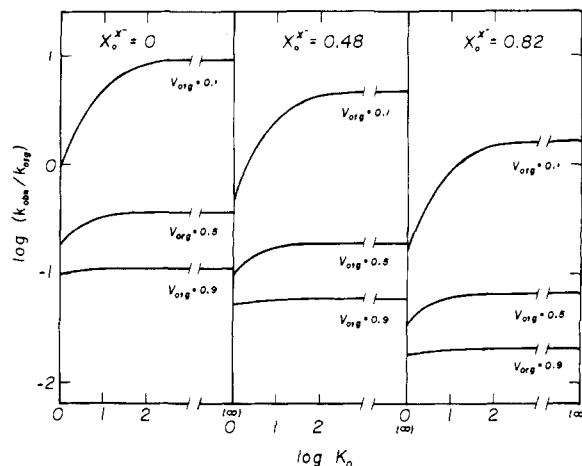
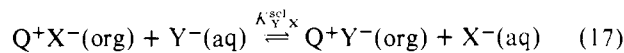
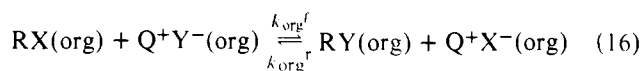


Figure 7. Catalytic efficiency vs. distribution coefficient of Q^+ (eq 15a).

The Reversible Second-Order Case. The liquid ion-exchange formulation is given by the equations



$$K = k_{\text{org}f}/k_{\text{org}r} \quad (19)$$

In most respects—obeyance of the second-order rate law only at $K_{Y/X}^{\text{sel}} = 1$, shape of the rate profile for $K_{Y/X}^{\text{sel}} \neq 1$, dependence of q_{phys} on the above parameters—this system is the same as the above. But the catalyst poisoning when $K_{Y/X}^{\text{sel}} < 1$ (Figure 2) becomes more acute in the reversible case, where depletion of $Y^-(\text{org})$ for the forward reaction is buttressed by accretion of $X^-(\text{org})$ for the reverse reaction, and there is a dependence of the equilibrium position on the PT parameters.

There is an apparent dependence of equilibrium position on the concentration of PT catalyst. Actually, the amount of catalyst is determining how much of the reaction proceeds from organic-phase and how much from aqueous-phase reactant and product states for the anions—two processes with definite but different equilibrium constants. When $c_0^{Q^+} = c_0^{Y^-}$ all ions are in the organic phase, and the equilibrium position is determined by K alone (Figure 8, extreme right). Decreasing the PT catalyst concentration, $c_0^{Q^+}$, shifts the reaction progressively to an aqueous reference state for the ions, and if water stabilizes Y^- more than X^- ($K_{Y/X}^{\text{sel}} < 1$) the equilibrium yield falls, as shown. If $K_{Y/X}^{\text{sel}} > 1$, the yield rises. The dependence of

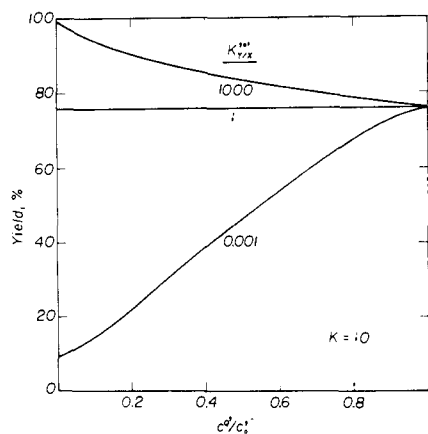


Figure 8. Percentage completion of reaction 18 vs. the fraction of initially present Y^- that is in the organic phase, for $K = 10$ (eq 16) and the $K_{Y/X}^{sel}$ values shown.

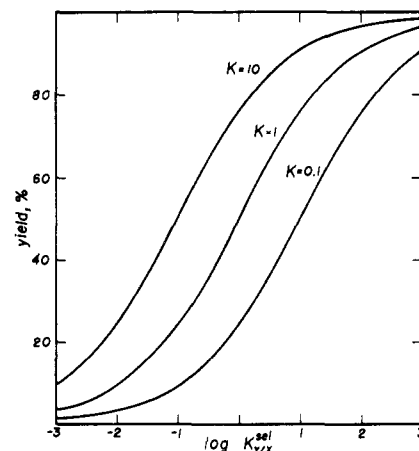


Figure 9. Percentage completion of reaction 18 vs. log selectivity coefficient (eq 3c) for three values of K (eq 16).

Table II. Details of the $RX + YH + OH^-$ Reactions Treated

	RBr + PhS ⁻¹⁰	RCl + BuO ⁻¹¹
Solvent	C ₆ H ₆	Tetrahydrofuran
PT catalyst	Q ⁺ Br ⁻	Q ⁺ HSO ₄ ⁻
Other added X ⁻ ?	No	Saturated with NaCl (~0.2 M)
OH ⁻ :RX	7.25:1	≥5:1
YH:RX	2.75:1	1:1
Expressions and equilibrium constants used		
YH(aq) + OH ⁻ (aq) = Y ⁻ (aq) + H ₂ O	+(K = 10 ⁸) ²⁰	
YH(aq) = YH(org)		+(K = ?) ^a
YH(org) + Q ⁺ OH ⁻ (org) = Q ⁺ Y ⁻ (org) + H ₂ O(aq)		+(K = 150) ^b
Y ⁻ (aq) + Q ⁺ OH ⁻ (org) = Q ⁺ Y ⁻ (org) + OH ⁻ (aq)	+(K = 0.68) ^c	
X ⁻ (aq) + Q ⁺ OH ⁻ (org) = Q ⁺ X ⁻ (org) + OH ⁻ (aq)	+(K = 9.5) ^c	+(K = 770) ^b
Y ⁻ (org) + OH ⁻ (org) + X ⁻ (org) = Q ⁺ (org)	+	+
Y ⁻ (aq) + Y ⁻ (org) + YH(aq) + YH(org) = 101al Y	+	+
X ⁻ (aq) + X ⁻ (org) + RX(org) = 101al X	+	+
OH ⁻ (aq) + OH ⁻ (org) = 101al OH ⁻	+	+

^a Unknown. $K \approx 6$ for pure water and (C₂H₅)₂O,²⁴ and it should be larger here due to salting out by NaCl and NaOH. Taken as ≥ 20 .
^b Calculated from data of ref 11. ^c Calculated from data of ref 10.

equilibrium position on $K_{Y/X}^{sel}$ at 1% PT catalyst is shown in Figure 9.

Systems Using Equilibrium Generation of Nucleophile. These include a number of systems of great practical importance (enolate alkylations, Williamson ether synthesis, etc). They introduce at least three new complications: the ion-exchange equilibrium of OH⁻ vs. Y⁻ and X⁻ (if OH⁻ is used to generate Y⁻ from YH), distribution of YH between the phases, and the YH = Y⁻ equilibrium. These additional equilibria can be incorporated in computerized numerical treatment of the kinetics without difficulty; new equilibrium concentrations of YH, Y⁻, X⁻, and OH⁻ in each phase must be calculated after each increment of RX + Y⁻ reaction. Sufficient data exist for a fairly complete treatment of two systems. Both are interesting in following second-order kinetics accurately despite the fact that $K_{Y/X}^{sel} \neq 1$ (cf. earlier discussion). Freedman's BuO⁻

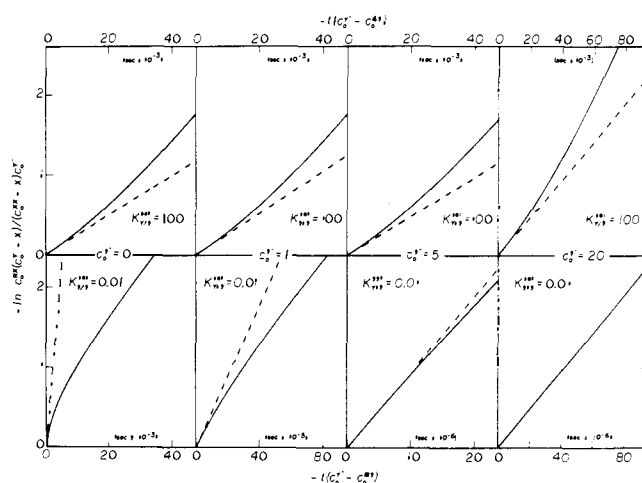


Figure 10. Rate profiles for reaction 1 in the presence of initially added product anion, plotted as second-order processes (solid curves). Dashed lines are extrapolations of the initial rate.

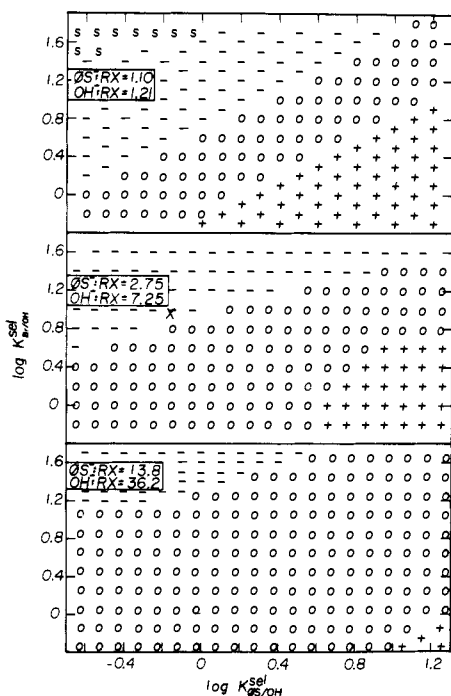
+ RCl reaction¹¹ uses an unusual medium (50% aqueous sodium hydroxide saturated with sodium chloride/tetrahydrofuran), but Herriott's PhS⁻ + RBr systems¹⁰ are straightforward. The conditions and the equations used to solve each system are summarized in Table II.

We first made a study of the effect of added product anion X⁻ to determine to what extent it might be expected to linearize second-order plots when $K_{Y/X}^{sel} \neq 1$. For $K_{Y/X}^{sel} < 1$ (but not for $K_{Y/X}^{sel} > 1$) added X⁻ straightens the curved second-order plots when it makes up about 90% (at $K_{Y/X}^{sel} = 0.01$) or 80% (at $K_{Y/X}^{sel} = 0.1$) of the initially present anions (Figure 10). These curves are not changed appreciably by using up to a 20-fold excess of OH⁻, so the excess of OH⁻ and the added Cl⁻ do not by themselves account for the good second-order kinetics observed in the RX/BuOH/THF system. However, modeling this system complete with the equilibria involving BuO⁻ gives rate profiles that are markedly sensitive to excess OH⁻ and Cl⁻. The results of roughly mapping the region of OH⁻:RCl and Cl⁻:RCl ratios giving clean second-order behavior are shown in Table III. With NaOH at about 19 M, NaCl about 0.2 M, RCl and *n*-C₄H₉OH equimolar and ≤ 1 M, the measurements were conducted well within the region of predicted linearity. Note that one easily steps outside that range by using fairly modest excesses of alcohol.

In the RBr + PhS⁻ reaction excess PhS⁻/OH⁻ has the same effect. Here we surveyed also the effect of the ion-exchange selectivity coefficients over a considerable range of

Table III. Effect of Excess OH⁻, Cl⁻, and *n*-C₄H₉OH on the Linearity of Second-Order Kinetic Plots for the System of Freedman and Dubois⁴

		<i>n</i> -C ₄ H ₉ OH/RCI			
		1.00	1.25		2.00
OH ⁻ : RCI	Cl ⁻ :RCI required for linearity	OH ⁻ : RCI	Cl ⁻ :RCI required for linearity	OH ⁻ : RCI	Cl ⁻ :RCI required for linearity
1	>20				
2	10				
5	0.2	5	>20	5	>20
10	None	10	10	10	15
20	None	20	5	20	10

**Figure 11.** Shape of standard second-order kinetic plots for the PhS⁻ + RBr reaction as a function of $K_{Br/OH}^{sel}$ and $K_{PhS/OH}^{sel}$: O, linear; +, concave up; -, concave down; S, sigmoid. Concentrations as shown.

values. These results are shown as maps of the shape of the rate profile as a function of $K_{PhS/OH}^{sel}$ and $K_{Br/OH}^{sel}$ in Figure 11. The center map is that obtained using the experimental concentrations of PhSH and OH⁻ used in the measurements of Herriott and Picker.¹⁰ The band of accurate second-order behavior (symbol: 0) is narrowed by decreasing and broadened by increasing the excess of PhS⁻ + OH⁻ (top and bottom maps, respectively). The values of $K_{PhS/OH}^{sel}$ and $K_{Br/OH}^{sel}$ calculated from preliminary distribution measurements of Herriott and Picker are plotted as an X in the center map. This lies just outside the predicted linear region. This may reflect the rough character of the distribution results, or it may just be due to use of a more stringent requirement for linearity in constructing the map from computed profiles (curvature visible when correlation coefficient $r = 0.998$) vs. that used in judging the experimental data ($r \geq 0.996^{10}$).

Summary

The treatment of PTC given here may prove useful in the following ways:

(1) Further work on mechanism and reactivity may require extraction of the chemical contribution to catalyst efficiency

by means equivalent to eq 12. Comparison of experiments involving different Q⁺ and/or M⁺ concentrations requires attention to this calculation.

(2) The illustrations given can serve as guidelines for the choice of systems for rate measurements that are likely to obey simple rate laws.

(3) While addition of a product anion to PTC experiments may serve specific purposes (e.g., linearization of second-order kinetic plots), Figure 6 shows that in preparative work one would want to avoid added X⁻ when $K_{Y/X}^{sel}$ is small.

(4) Foreign anions are unavoidable in equilibrium generation of nucleophiles (e.g., via $YH + OH^- \rightleftharpoons Y^- + H_2O$), and they can be used to simplify PTC kinetics (e.g., Table III); but they depress the rate by competing with Y⁻ for organic-phase anionic sites. In this context OH⁻ is a good base because $K_{OH/Y}^{sel}$ values tend to be low (OH⁻ rejected by the organic phase; Figure 2). However, more lipophilic/less hydrophilic anions (e.g., alkoxides) may prove less satisfactory as a result of larger $K_{RO/Y}^{sel}$ values.

(5) Seeing PTC as liquid ion-exchange catalysis suggests a possible means of combating catalyst poisoning, namely buttressing the PT catalyst with larger amounts of a solid ion-exchange resin, res⁺Y⁻. This would work best if the resin's $K_{Y/X}^{sel}$ were smaller than the catalyst's. The common resins have $K_{Y/X}^{sel}$ orders and magnitudes²³ similar to those of the Q⁺ liquid exchangers (Figure 2), but they still may be effective. Buttressing with near stoichiometric quantities of resin sounds at first like defeating the purpose of PTC, however the insoluble resin is more easily recovered and regenerated than the soluble catalyst.

Computation

The stoichiometric conversion of $RX + Y^-$ into $RY + X^-$ was caused to occur in n increments. At the midpoint of each increment new values of Y⁻ and X⁻ were computed, then the ion-exchange equilibrium, mass- and charge-balance expressions, and (if present) subsidiary equilibria were solved simultaneously for $c_{org}^{Y^-}$. A mean rate for the increment was obtained from the current $c_{org}^{Y^-}$, c_{org}^{RX} , and eq 7 (or analogue). From the rate and the width of the concentration increment, c_0^{RX}/n , the time increment, Δt , was computed. Y⁻, X⁻, and RX were incremented, and the cycle was repeated. Output was a table of c_{org}^{RX} vs. t . $n = 50$ gave smooth results. Such results were used: (a) to prepare Figures 3, 4, and 10; (b) to determine conditions under which linear kinetic plots are observed (Tables I and III, Figure 11); (c) to verify eq 10-15. For this purpose k_{obsd} was obtained from linear second-order, or linear pseudo-first-order plots, or from initial rates, depending upon the form of the profile. For extrapolation of initial rates the first ten points of a run with $n = 500$ were examined in some cases.

In the reversible second-order case the equilibrium composition was first solved by numerical means. The kinetic problem was treated as above, using as rate law: rate = $k_{\text{org}}^f c_{\text{org}}^{\text{RX}} c_{\text{org}}^{\text{Y}^-} - k_{\text{org}}^r c_{\text{org}}^{\text{RY}} c_{\text{org}}^{\text{X}^-}$.

References and Notes

- (1) Presented in part in the Symposium on Phase-Transfer Catalysis, 8th Central Regional Meeting, American Chemical Society, Akron, Ohio, May 20, 1976.
- (2) C. M. Starks, *J. Am. Chem. Soc.*, **93**, 195 (1971).
- (3) The number of possible models increases substantially if one includes ancillary equilibria (ion-association, micelle-formation, ion-solvation equilibria). While it is true that some of these equilibria undoubtedly perturb the selective distribution of anions between the phases,⁴ data do not exist to parametrize them for the PTC systems of interest. These effects, if present, are however included in the experimental liquid ion-exchange selectivity coefficients whose use in correlating PTC is advocated in this paper. Consequently, omission of ion-association equilibria, etc., may be expected to limit the ranges of concentrations for accurate application of the expressions derived, but to have little effect on qualitative differences in behavior of individual ions as predicted via $K_{Y/X}^{\text{sel}}$.
- (4) A. Brändström, "Preparative Ion-Pair Extraction", Apotekarsocieteten/Hälsle. Läkemedel, Sweden, 1974.
- (5)
$$\begin{array}{c} \text{RX} + \text{Q}^+\text{Y}^- \longrightarrow \text{RY} + \text{Q}^+\text{X}^- \text{ (organic phase)} \\ \text{-----} \uparrow \qquad \qquad \qquad \downarrow \text{-----} \\ \text{M}^+\text{X}^- + \text{Q}^+\text{Y}^- \rightleftharpoons \text{M}^+\text{Y}^- + \text{Q}^+\text{X}^- \text{ (aqueous phase)} \end{array}$$
- (6) C. M. Starks and R. M. Owens, *J. Am. Chem. Soc.*, **95**, 3613 (1973).
- (7) (a) F. Helfferich, "Ion Exchange", McGraw-Hill, New York, N.Y., 1962; (b) E. F. Caldin, "Fast Reactions in Solution", Wiley, New York, N.Y., 1964.

- (8) Conditions used are those for early stages of the $\text{RBr} + \text{Br}^-$ reaction in $\text{H}_2\text{O}/\text{CHCl}_3$ with $\text{Q}^+ = \text{Bu}_4\text{N}^+$, $E_{\text{QY}} = 19.5$,⁴ organic-phase K_{assn} for Q^+Y^- large, and aqueous-phase K_{assn} for $\text{Q}^+\text{Y}^- = 5$.²¹ Aqueous-phase concentrations: Q^+ , 3.9×10^{-4} ; Y^- , 0.99; X^- , 10^{-3} ; Q^+Y^- , 2.0×10^{-3} M. Organic-phase concentration: Q^+Y^- , 7.5×10^{-3} M. Organic solvent droplet radius = 10^{-2} – 10^{-1} cm. Droplet surface film thickness = 5×10^{-3} cm.
- (9) J. Koryta, "Ion-Selective Electrodes", Cambridge University Press, Cambridge, 1975, p 64.
- (10) A. W. Herriott and D. Picker, *J. Am. Chem. Soc.*, **97**, 2345 (1975).
- (11) H. H. Freedman and R. A. Dubois, *Tetrahedron Lett.*, 3251 (1975).
- (12) (a) Reference 7a, Chapter 11; (b) J. E. Gordon, *J. Chromatogr.*, **18**, 542 (1965); (c) C. H. Chen and L. P. Hammett, *J. Am. Chem. Soc.*, **80**, 1329 (1958), and previous papers.
- (13) E. Högföldt in "Ion Exchange", Vol. 1, J. A. Marinsky, Ed., Marcel Dekker, New York, N.Y., 1966, Chapter 4.
- (14) H. J. James, G. P. Carmack, and H. Freiser, *Anal. Chem.*, **44**, 853 (1972).
- (15) R. P. Buck, *Anal. Chem.*, **44**, 270R (1972); **46**, 28R (1974); **48**, 23R (1976).
- (16) (a) J. W. Ross, *Natl. Bur. Stand. Spec. Publ. No. 314*, Chapter 2 (1969); (b) M. S. Frant, private communication, 1976.
- (17) C. J. Coetzee and H. Freiser, *Anal. Chem.*, **41**, 1128 (1969).
- (18) (a) T. Stwerczewicz, J. Czapkiewicz, and M. Leszko, "Ion-Selective Electrodes", E. Pungor, Ed., Akademiai Kiado, Budapest, 1973, p 259; (b) J. E. Gordon, "The Organic Chemistry of Electrolyte Solutions", Wiley, New York, N.Y., 1975, sections 1.II.B, 2.IV, 2.VI, 3.III.
- (19) L. P. Hammett, "Physical Organic Chemistry", McGraw-Hill, New York, N.Y., 1970, p. 16.
- (20) H. Morawetz, *Adv. Catal.*, **20**, 341 (1969).
- (21) Reference 18, pp 465 f.
- (22) A. Albert and E. P. Serjeant, "The Strengths of Organic Acids and Bases", Methuen, London, 1962.
- (23) Y. Marcus and A. S. Kertes, "Ion Exchange and Solvent Extraction of Metal Complexes", Wiley, New York, N.Y., 1969.
- (24) A. Leo, C. Hansch, and D. Elkins, *Chem. Rev.*, **71**, 525 (1971).

Symmetry Considerations and Correlation Diagrammatic Analyses of Certain Photochemical Reactions with and without Spin Inversion

Tieh-sheng Lee

Contribution from the Chemistry Department, National Chung Hsing University, Taichung, Taiwan, Republic of China. Received April 2, 1976

Abstract: When studying the electronic radiationless transitions of molecular systems in general, Lin obtained a set of symmetry selection rules in 1966 by considering the symmetry features of the set of promoting modes involved. The rules read: $\Gamma(\phi_a^0)\Gamma(Q_i)\Gamma(\phi_b^0) = A$; $\Gamma(\phi_a^0)\Gamma((\partial h_{so}/\partial Q_i)_0)\Gamma(\phi_b^0) = A$; $\{\Gamma(\phi_a^0)\Gamma((\partial h_0/\partial Q_i)_0)\Gamma(\phi_c^0)\}\Gamma(\phi_c^0)\Gamma(h_{so}^0)\Gamma(\phi_b^0) = A$; $\{\Gamma(\phi_a^0)\Gamma(h_{so}^0)\Gamma(\phi_c^0)\}\Gamma(\phi_c^0)\Gamma((\partial h_0/\partial Q_i)_0)\Gamma(\phi_b^0) = A$; where the letter A stands for the phrase, "the totally symmetric species of the point group of interest" and $\Gamma(\xi)$ denotes the symmetry representation of the argument ξ , which may either be a function or an operator. It has been demonstrated in this article that the rules of Lin can be applied equally well to a large body of chemical reactions if certain slight modifications of the rules are introduced. In dealing with chemical reactions, if molecular systems are described by wave functions in the Born–Oppenheimer approximation, the wave function of the reacting system may take the form of the superposition of various such adiabatic wave functions with time-dependent coefficients. Chemical reactions can then be viewed as the transitions from the initial molecular systems to the final ones due to the breakdown of the Born–Oppenheimer approximation. This enables one to treat chemical reactions just the same way as Lin did for radiationless transitions and the same set of symmetry selection rules must be applicable. The verification of the applicability of this set of rules is explicitly demonstrated by studying a number of photochemical reactions. A systematic procedure for the symmetry analysis for chemical reactions in general is thus developed. This involves the examination of the orbital symmetries based on the newly proposed rules, the construction of the orbital correlation diagram, and the detection of the presence of a particular diagrammatic topology associated with the orbital avoided crossing. Results are promising. The Woodward–Hoffmann type symmetry conservation rules are found to be merely special cases. Reactions involving spin inversion can likewise be systematically analyzed so that the different behavior of the photochemically excited singlet and triplet states of various organic compounds can be better understood. Most importantly, the avoided surface crossing concept Salem originally discussed has been investigated by using the promoting mode concept of Lin. It has been found that when dealing with transitions involving open-shell states, the use of the MO energies obtained by the unrestricted Hartree–Fock wave function approach gives results different from those of Salem's in certain cases.

Symmetry-based selection rules for chemical reactions have now become a research interest that receives an increasing popularity since the publication of a series of communications of Woodward and Hoffmann.^{1–3} Reactions analyzed by their

approach included the electrocyclic type, the sigmatropic type, and the concerted cycloaddition type. This well-known orbital-symmetry conservation concept was extended to deal with transition metal catalytic reactions first by Mango and